Rev. Adv. Mater. Technol., 2022, vol. 4, no. 1, pp. 1–8 DOI: 10.17586/2687-0568-2022-4-1-1-8

Recent Progress in Contact Mechanics Methods for Solids with Surface Roughness Using Green's Function Molecular Dynamics

I. Solovyev[1], V. Petrenko[1], Y. Murugesan[2], L. Dorogin[1]

[1] Saint Petersburg National Research University of Information Technologies, Mechanics and Optics (ITMO University), St. Petersburg, 197101, Russia
[2] Department of Industrial Engineering, University of Padova, I-35131, Italy

Article history

Received February 11, 2022
Accepted February 27, 2022
Available online March 27, 2022

Abstract

In spite of importance of tribology of solids with surface roughness, there is no synthesized theory covering adhesion yet. One of the methods to describe adhesion in tribological systems is the Green's Function Molecular Dynamics (GFMD). This work aims at reviewing the most recent GFMD techniques and applications of GFMD in contact mechanics. There are different attributes of this method that are important for its realization: model to describe surface roughness, model to describe interfacial forces, constitutive model to describe the solid deformation and algorithm to minimize surface potential energy. We organize this review using the following set of parameters: degrees of freedom of the system modelled, substrate geometry, loading control, material properties, surface topography, interfacial interaction models.

Keywords: Contact mechanics; Surface roughness; Green's function molecular dynamics; Adhesion; Friction

1. INTRODUCTION

Tribology has begun to interest scientists since the early times of Leonardo da Vinci, Coulomb and many more. Tribology of soft materials plays a crucial role in natural, biological and technological systems. In spite of its importance and the efforts of scientists, this topic is still only partially understood. There are biological systems, such as insects, tree frogs and Geckos, having hierarchically-structured adhesive pads from elastically stiff materials (keratin-like proteins) that appear macroscopically soft, and allow the animals to adhere even to very rough surfaces [1]. This complex interplay of surface topography and adhesion plays a huge role in industrial design, where soft materials are one of the essential components.

Weak forces acting between atoms in solids could appear strong on the macroscopic scale, but surface roughness can change it. Surface roughness reduces the actual area of contact, leads to local deformation of roughness asperities and results in nearly vanishing adhesion pull-off forces in most practical case. However, for soft elastic solids, e.g., rubber, on smooth surfaces adhesion can be noticeable at the macroscopic scale.

The non-adiabatic effects can result in an adhesion force that is much weaker during approach compared to pull-off which is called adhesion hysteresis. Adhesion hysteresis is in general a function of contact history, e.g., maximum loading force and contact duration. For instance, for smooth surfaces, where the contact is complete, we expect only weak dependency of the pull-off force on the maximum loading force. At the same time adhesion hysteresis can be strongly "multiplied" by numerous contact zones as was shown in Ref. [2]. However, the work of adhesion of a contact with a rough surface can be increased with increasing maximum preload force [3]. Finally, three major contributions to adhesion acting at different length scales can be distinguished: bulk mechanical response, roughness and molecular mobility. Those three contributors require individual mathematical apparatus to be described. For instance, to describe molecular mobility binding cohesive zone models (CZM) could be used (see the CZM section below), bulk mechanical response could be treated as constitutive material law (Hooke's law for elastic and Maxwell-Zener model for viscoelastic material), whereas roughness could be mathematically fully described by the grid of elements (in boundary element methods and finite element methods) or

* Corresponding author: I. Solovyev, e-mail: ivaso@yandex.ru

could be accounted using the set of statistical parameters. One of the methods to describe such adhesion in tribological systems is the Green's Function Molecular Dynamics (GFMD). GFMD is a boundary element method (BEM) allowing one to simulate the response of a linear solid with elastic or viscoelastic properties to an external stress and to a boundary condition. The main advantage of GFMD technique is that it only requires knowledge of the displacements in the boundary of a solid and that effective interactions have diagonal tensors in Fourier space. Therefore, relatively large systems can be simulated and be quickly relaxed. Contact mechanics is one of the major and most challenging problems of materials science. The state of the real surfaces in contact is difficult to define due to the surface roughness and adhesion heavily affecting contact phenomena. This article focuses on reviewing recent GFMD techniques and applications, especially in the field of adhesive viscoelastic interactions.

2. SURFACE TOPOGRAPHY

Surface topography plays an important role in a multitude of physical and tribological phenomena such as contact mechanics, friction, adhesion, wear, wettability, lubrication, etc. Surface topography causes discrete contact points, when two rough nominally flat surfaces are brought together; the real area of contact is the accumulation of the area of the individual contact points. There are different real surfaces types obtained by manufacturing, which are associated with certain process: turning, grinding, polishing and deburring. For example, a machined surface produced by a lathe has a regular structure associated with the depth of cut and feed rate, but the heights of the ridges still show some statistical variations.

The most common real surface topography measurement methods are:

1. Stylus profilometers (2D+1D);
2. Optical methods (3D) – Interferometry;
3. Scanning probe microscopy (2D+1D);
    a. Scanning tunneling microscopy (STM),
    b. Atomic force microscopy (AFM).

These experimental methods allow extracting certain data of the real surfaces. The most common parameters are: height profile (1D is a line profile, 2D – scan, 3D – interferogram), average roughness R_a,

$$R_a = \frac{1}{L}\int_0^L \left| y(x) \right| dx. \tag{1}$$

Here $y(x)$ is a function of a height profile, L is the length of the studied surface. Root mean square (RMS) roughness R_q:

$$R_q = \sqrt{\frac{1}{L}\int_0^L y(x)^2 \, dx}, \tag{2}$$

RMS slope Δq:

$$\Delta q = \sqrt{\frac{1}{L}\int_0^L \left(\frac{d\,y(x)}{d\,x} \right)^2 dx}. \tag{3}$$

It could be noted that real surface topography measurements are never exact and extracted parameters are statistically dependent.

3. FRACTAL-BASED RANDOM ROUGHNESS

There are number of approaches to generate random surfaces. One of them is generation of random rough surface through the means of fractal geometry. It is known that surface topography is a nonstationary random process where the variance of the height of distribution is related to the length of the sample. The fractal approach is based on the observation that the morphology of surfaces is statistically self-affine, which implies that when repeatedly magnified, increasing details of roughness emerge and appear similar to the original profile. With the fractal approach, it is possible to calculate the scale-independent parameters, which describe the surface [4].

The first one is a roughness parameter or Hurst exponent of roughness H. The Hurst exponent is referred to as the "index of dependence" or "index of long-range dependence". For self-affined structures H is directly related to fractal dimension D, where $1 < D < 2$, such that $D = 2 - H$. The values of the Hurst exponent vary between 0 and 1, with higher values indicating a smoother trend, less volatility, and less roughness [5].

The second parameter is an intrinsic parameter called the fractal dimension of surface: D ($1 < D < 2$) or D_s ($2 < D_s < 3$). It represents the capacity of the surface to fill in the adjacent volume.

Kanafi [6] used the fractal geometry approach to generate artificial randomly rough isotropic surfaces. The code was based on simulating the surface topography/roughness by means of fractals. It uses the Fourier concept (specifically the power spectral density) for surface generation. The power spectral density (PSD) of a surface is a mathematical tool that decomposes a surface into contributions from different spatial frequencies (wavevectors). Definition of the PSD used by B. Persson [7] is:

$$C(\boldsymbol{q}) = \int_A \left\langle h(\boldsymbol{x}) h(0) \right\rangle e^{-i\boldsymbol{q}\boldsymbol{x}} d^2\boldsymbol{x}, \tag{4}$$

where A is the surface area under study, $\boldsymbol{q}$ is a wavevector, $\boldsymbol{x} = (x, y)$ and $h(\boldsymbol{x})$ is a height of the substrate measured from the average surface plane.

Mathematically, PSD is the Fourier transform of the autocorrelation function of the signal, which contains just

the power (and not the phase) across a range of wavevectors [8]. This allows identification of the spatial frequencies that can be found in the signal. The most recent methods of computing random surface parameters (RMS height, slope, and curvature) using the PSD method were reviewed in Ref. [9].

Main parameters in the Kanaffi method [6] are:

1. s_d – standard deviation of surface heights;
2. H – Hurst exponent, which is related to the fractal dimension of a surface topography $D = 2 - H$. For example, a Brownian surface roughness has $H = 0.5$. The parameter H can take values between 0 and 1;
3. L_x – length of final topography/image in x direction (it could take any values from nanometer to hundreds of meters);
4. (Optional) q_r – roll-off wavevector.

The input (0.001, 0.8, 0.1, 1000) generates a surface (see Fig. 1 and Fig. 2) with standard deviation of 1 mm, Hurst exponent of 0.8 (i.e., fractal dimension of 2.2), length of final image is 10 cm. It generates a rectangular image with 1024 data points in x direction and 512 data points in y direction. The surface has a roll-off region at $q_r = 1000$ m^{-1}, which equals to a wavelength $\lambda_r = 2\pi / q_r = 6.3$ mm.

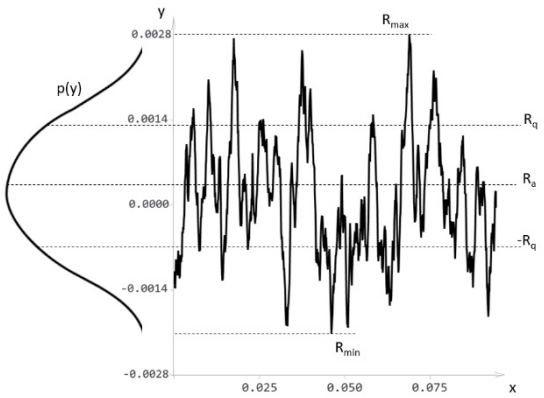

Fig. 1. Representation of the height profile of a randomly generated rough surface with associated height distribution function $p(y)$, maximum height $R_{\max}$, minimum height $R_{\min}$ and RMS height R_q.

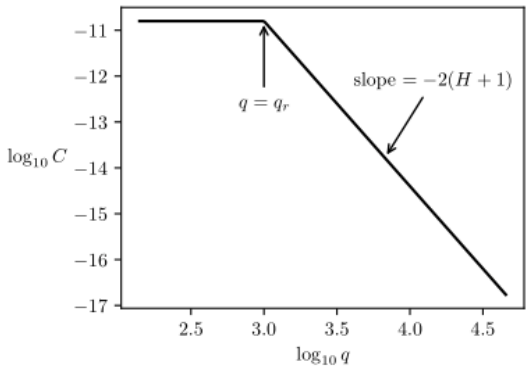

Fig. 2. Illustration diagram of power spectrum of a surface topography with Hurst exponent $H = 0.8$ and cut-off wavevector $q_r = 1000$.

4. INTERFACIAL FORCES, ADHESION, COHESIVE ZONE MODELS

As the surfaces (known as cohesive surfaces) separate, traction first increases until a maximum is reached, and then subsequently reduces to zero which results in complete separation. CZM maintains continuity conditions mathematically. It eliminates singularity of stress and limits it to the cohesive strength of the material.

The cohesive constitutive relationships can be classified as either nonpotential-based models or potential-based models. Nonpotential models do not guarantee consistency of the constitutive relationship for arbitrary mixed-mode conditions, because they do not account for all possible separation paths. For potential-based models, the traction-separation relationships across fracture surfaces are obtained from a potential function, which characterizes the fracture behavior.

4.1. Dugdale potential

Dugdale [10] employed a cohesive zone model to investigate yielding at a crack tip and size of the plastic zone in a steel sheet. The cohesive traction along the cohesive zone was assumed to be constant when the separation is smaller than a critical value. The cohesive law is then given by

$$\sigma = \begin{cases} \dfrac{\phi}{\delta_n}, & \text{if } \delta > 0 \text{ and } \delta < \delta_n, \\ 0, & \text{otherwise.} \end{cases} \tag{5}$$

where σ is a stress, δ is a separation distance, δ_n is a cut-off distance. Here ϕ is the work of adhesion:

$$\phi = \int_0^\infty \sigma \, d\delta. \tag{6}$$

Since the cohesive traction is constant, we need to specify a potential energy density E. The relation between them is

$$E = \int \sigma \, d\delta, \quad \text{if } \delta > 0 \text{ and } \delta < \delta_n, \tag{7}$$

$$E = \begin{cases} \phi \dfrac{\delta - \delta_n}{\delta_n}, & \text{if } \delta > 0 \text{ and } \delta < \delta_n, \\ 0, & \text{otherwise.} \end{cases} \tag{8}$$

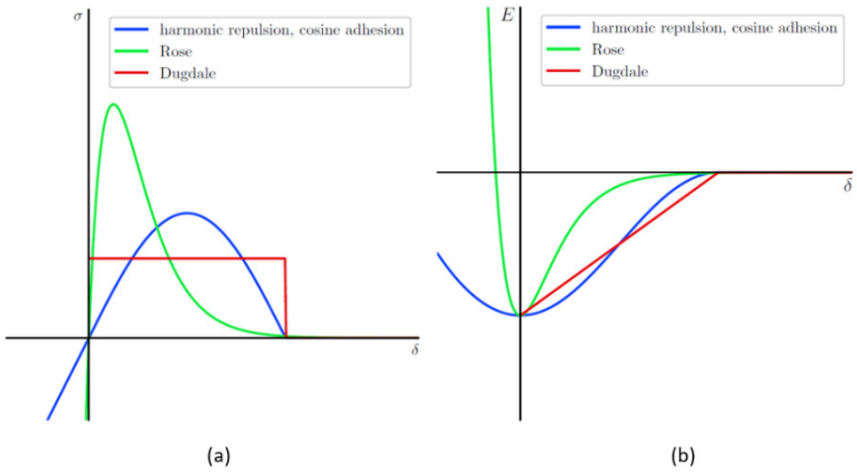

(a) (b)

Fig. 3. Plot of stress σ (a) and potential energy (b) as a function of separation δ for the Dugdale, Rose, and cosine adhesion models.

Using the Dugdale model to simulate fracture propagation, complete separation of materials occurs when $\delta = \delta_n$ (see Fig. 3).

4.2. Rose potential

Rose et al. [11] studied crack growth in ductile metals. They introduced an exponential cohesive zone model based on the universal binding energy curve from the atomistic consideration. In this model the equation for the stress takes an exponential form:

$$\sigma = \frac{\phi}{\delta_n^2} e^{-\frac{\delta}{\delta_n}} = \sigma_c \frac{\delta}{\delta_n} e^{1-\frac{\delta}{\delta_n}}, \tag{9}$$

where σ_c is the peak cohesive traction, which occurs in the separation displacement point. Then potential energy density could be found as

$$E = \phi\left(-\frac{\delta}{\delta_n} - 1\right) e^{-\frac{\delta}{\delta_n}}. \tag{10}$$

4.3. Harmonic repulsion. Cosine adhesion

Another approach to the simulation of the crack propagation in materials is the cosine adhesion. Binding forces could be found as:

$$\sigma = \begin{cases} \sqrt{\frac{p\phi}{2}} \sin\sqrt{\frac{2p}{\phi}}\delta, & \text{if } \delta > 0 \text{ and } \delta < \delta_n, \\ \delta p, & \text{if } \delta < 0, \\ 0, & \text{otherwise,} \end{cases} \tag{11}$$

where p is curve parameter. It is equal to tangent of angle between the line under condition $\delta < 0$ and δ axis and could be also expressed as

$$p = \frac{\phi\pi^2}{2\delta_n^2}. \tag{12}$$

Then potential energy density could be found as

$$E = \begin{cases} -\frac{\phi}{2}\left(1 + \cos\sqrt{\frac{2p}{\phi}}\delta\right), & \text{if } \delta > 0 \text{ and } \delta < \delta_n, \\ -\phi + \frac{p\delta^2}{2}, & \delta < 0, \\ 0, & \text{otherwise.} \end{cases} \tag{13}$$

The potential energy and force of the discussed cohesive zone models are shown in Fig. 3.

Fig. 4 shows interfacial forces between a rigid cylindrical indenter and an elastic half-space. The cohesive zone model used here is cosine adhesion. Crack tip is a point where interfacial forces compensate each other and contact happens.

5. PRINCIPLE OF THE GFMD ALGORITHM FOR A GENERIC SYSTEM

The central aspects of the approach are described as follows. We denote the position of surface points facing the substrate by their lateral and normal coordinates, which are equally spaced on a two-dimensional surface (for a 3D case) or on a line (in case of 2D), representing $N = n \times n$ grid points. In-plane periodic boundary conditions are employed and the system is treated as being homogeneous within the plane. The coordinate system is chosen with the initial position of non-deformed substrate at zero z-coordinate. The grid points are propagated in time according to Newton's equation of motion, which is achieved with the Verlet algorithm. The quasi-static solution at time $t_n + \Delta t$ is obtained by solving the equation of motion for each mode with a unit mass in reciprocal space over a

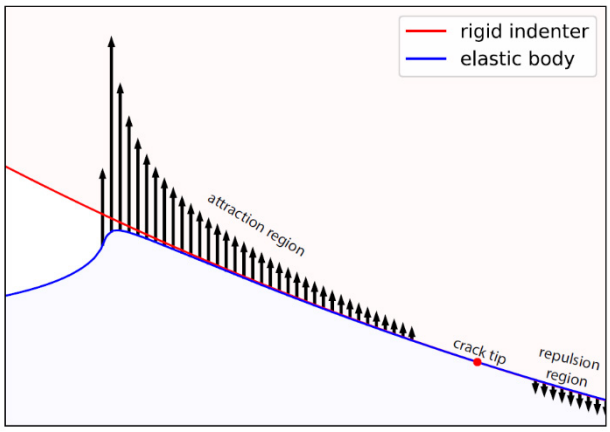

Fig. 4. Interfacial forces between a rigid cylindrical indenter and an elastic half-space. The cohesive zone model is cosine adhesion.

dimensionless time-step Δt^*. The quickest way to find quasi-static solution is critically damping each mode in reciprocal space [12]. Overdamping of the equation of motion is prevented through a non-monotonous adiabatic critical damping coefficient. It can be ensured that the energy minimum is reached and the computational time is minimized by using dynamic energy minimization in GFMD simulations. An analytical expression for the critical damping coefficient and the equilibrium time can be derived for the certain GFMD system to minimize the computational time.

The total normal force, F_i, acting on a grid point is the sum of an external force, the elastic force, a damping force, and interfacial force. The external force is either a constant or normalized according to mass center of substrate located in $z = 0$. The elastic restoring force on each atom is computed from the Fourier transform of the stress in Fourier space. Interfacial forces depend on the chosen CZM and potential model (Rose, Dugdale, etc.).

5.1. Generalized pseudo-code of a GFMD simulation

1. Let $\boldsymbol{h}$ be the surface topography of the punch.
2. Let Δt be the time step.
3. Let DFT be the discrete Fourier transform.
4. Determine damping factor vector $\boldsymbol{\eta}$.
5. Loop until converged:
   (a) calculate elastic force:
   $\boldsymbol{F} \leftarrow \mathrm{DFT}^{-1}(\mathrm{function}\{\mathrm{DFT}(\boldsymbol{u})\})$;
   (b) add external force and interfacial force:
   $\boldsymbol{F} \leftarrow \boldsymbol{F}_{\mathrm{external}} + \boldsymbol{F}_{\mathrm{interfacial}}(\boldsymbol{u},\boldsymbol{h})$;
   (c) add damping forces:
   $\boldsymbol{v} \leftarrow (\boldsymbol{u} - \boldsymbol{u}_{\mathrm{old}})/\Delta t$,
   $\boldsymbol{F} \leftarrow \boldsymbol{F} + \mathrm{DFT}^{-1}(\boldsymbol{\eta} \odot \mathrm{DFT}(\boldsymbol{v}))$,
   where $\odot$ denotes elementwise multiplication;
   (d) use Verlet to update the surface displacement vector $\boldsymbol{u}$:
   $\boldsymbol{u}_{\mathrm{new}} \leftarrow 2\boldsymbol{u} - \boldsymbol{u}_{\mathrm{old}} + \boldsymbol{F}\Delta t^2$,
   $\boldsymbol{u}_{\mathrm{old}} \leftarrow \boldsymbol{u}$,
   $\boldsymbol{u} \leftarrow \boldsymbol{u}_{\mathrm{new}}$.

The dominant operation in the convergence loop is the discrete Fourier transform, which can be computed in $O(n \log n)$ time (see the next subsection). Thus, the time complexity of the algorithm is $O(m\, n \log n)$, where m is the number of iterations of the convergence loop and n is the number of points on the surface of the elastic body. Note that each vector operation in the convergence loop except DFT is trivially parallelizable.

5.2. Computational efficiency of fast Fourier transform

A fast Fourier transform (FFT) is an algorithm that computes the DFT in $O(n \log n)$ time, where n is the data size. In order to compute the DFT in a GFMD simulation efficiently, the following FFT implementations can be used:

- single-threaded fastest Fourier transform in the west (FFTW) [13];
- multi-threaded FFTW with OpenMP;
- distributed-memory FFTW with MPI;
- cuFFT on an NVIDIA GPU.

Table 1 and Fig. 5 show how much time it takes to do a forward and backward 1D double-precision FFT. The time varies with data size in each implementation. This benchmark was performed on a laptop with a dual-core Intel Core i5-4200M 2.50 GHz CPU and NVIDIA GeForce GT 740M GPU.

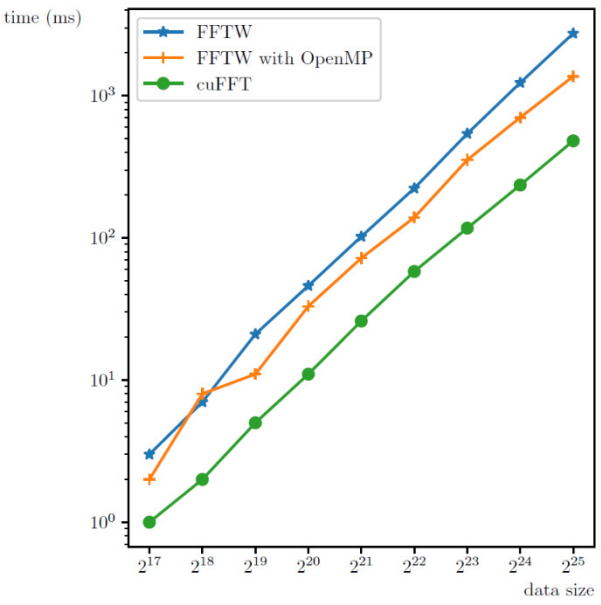

Fig. 5. Plot of the FFT running time as a function of array size for FFTW, FFTW with OpenMP, and cuFFT.

Table 1. Fast Fourier transform efficiency tests (runtimes are given in milliseconds).

Data size	FFTW	FFTW OpenMP 4 threads	FFTW MPI 4 processes	cuFFT
2^{17}	3	2	6	1
2^{18}	7	8	15	2
2^{19}	21	11	35	5
2^{20}	46	33	74	11
2^{21}	102	72	159	26
2^{22}	223	139	329	58
2^{23}	540	353	685	117
2^{24}	1232	702	1442	235
2^{25}	2739	1366	2896	481

6. RECENT GFMD METHODS AND APPLICATIONS FOR CONTINUUM CONTACT MECHANICS

In Table 2 recent GFMD methods and applications for continuum contact mechanics are presented. In 2007 Campana et al. [14] showed that GFMD tool could be used effectively to solve problems of continuum contact mechanics. Being one of the first works of this kind, it naturally considered a simple case of rough elastic isotropic half-space plane and smooth indenter interaction. Prodanov et al. [12] summarized the understanding of GFMD conception and obtained relations for majority of the necessary parameters of 2D elastic systems.

The first work to describe finite-thickness systems using GFMD technique appear to be Ref. [15]. They extended GFMD method to compute contact pressures and surface displacements of finite elastic smooth solids with generic Poisson's ratio and boundary conditions. This extension allowed the GFMD technique to provide the same information that can be obtained through the FEM, but with a significant gain in simulation time. In 2019 the work was extended for the case of a rough substrate [16]. Later in 2021 Venugopalan et al. [17] focused on two aspects of 3D finite-thickness systems: the subsurface stresses induced by contact between rough surfaces and the effect of compressibility of the bodies on those stresses.

Salehani et al. [18] showed how to extend GFMD on adhesive frictional contacts of elastically deformable solids under mixed-mode loading. The novelty of this model lies in its capability of studying the variation of contact area and of the friction force before and after the onset of sliding, under compressive or tensile loading.

In Ref. [19] GFMD method was further extended and also the semi-analytical method was implemented to obtain fast and accurate solution of the equations of motion to predict the transient and steady-state response of frictionless contacts. This method was applied to study the frictionless indentation and rolling of a smooth infinitely long rigid cylinder on a viscoelastic half-plane. This problem was further investigated in Refs. [20] and [21].

Table 2. Recent applications of GFMD stating their basic model parameter set. Abbreviations: Half-space plane = HS, Finite thickness = Zm, Pressure controlled = PC, Displacement controlled = DC, Experimental roughness = ER, Synthesized roughness = SR.

Author	2D/3D	Displacement dimension	Geometry	Type of control	Material properties	Surface topography	Interactions/CZM
Campana et al. (2007) [14]	2D	1D	HS	PC	Elastic, isotropic	ER	Hard-wall
Prodanov et al. (2014) [11]	2D	1D	HS	PC	Elastic, isotropic	SR	Hard-wall
Venugopalan et al. [15]	3D	1D	Zm	DC	Elastic, anisotropic/isotropic	Smooth	Hard-wall
Venugopalan et al. 2019 [16]	3D	1D	Zm	PC	Elastic/Plastic isotropic	SR	Hard-wall
Murugesan et al. [17]	3D	1D	Zm	DC	Elastic, isotropic	SR	Hard-wall
Salehani et al. [18]	2D	2D	HS	DC	Elastic, isotropic	Smooth	Rose
Dokkum et al. 2018 [19]	2D	1D	HS	PC	Elastic anisotropic	SR	Non-adhesive contact
Dokkum et al. 2019 [20]	2D	1D	HS	DC	Viscoelastic Zener, isotropic	Smooth	Hard-wall
Dokkum et al. 2021 [22]	2D	2D	HS	DC	Viscoelastic Zener, isotropic	Smooth	Dugdale
Sukhomlinov et al. 2021 [21]	2D	2D	HS	PC	Viscoelastic Kelvin-Voigt	SR	Cosine repulsion, Dugdale

7. CONCLUSIONS

In this paper, we review the pivotal aspects of the GFMD contact mechanics methods: representation of surface topography, interfacial models, main principles of GFMD computational algorithm. Additionally, the recent state of the art GFMD methods are reviewed and organized by the set of input parameters namely: degrees of freedom of the system modelled, substrate geometry, loading control, material properties, surface topography, interfacial interaction used. This review can serve as a reference map for extending contact mechanical models for more accurate predictions of tribological properties of realistic contact mechanical systems.

ACKNOWLEDGEMENTS

This work was supported by the Ministry of Science and Higher Education of the Russian Federation (agreement nr. 075-15-2021-1349).

REFERENCES

[1] B.N.J. Persson, S. Gorb, *The effect of surface roughness on the adhesion of elastic plates with application to biological systems*, The Journal of Chemical Physics, 2003, vol. 119, no. 21, pp. 11437–11444.

[2] L. Dorogin, A. Tiwari, C. Rotella, P. Mangiagalli, B.N.J. Persson, *Role of preload in adhesion of rough surfaces,* Phys. Rev. Lett., 2017, vol. 118, no. 23, art. no. 238001.

[3] A. Tiwari, L. Dorogin, A.I. Bennett, K.D. Schulze, W.G. Sawyer, M. Tahir, G. Heinrich, B.N.J. Persson, *The effect of surface roughness and viscoelasticity on rubber adhesion*, Soft Matter, 2017, vol. 13, no. 19, pp. 3602–3621.

[4] H. Zahouani, R. Vargiolu, J.-L. Loubet, *Fractal models of surface topography and contact mechanics*, Mathematical and Computer Modelling, 1998, vol. 28, no. 4, pp. 517–534.

[5] T. Gneiting, M. Schlather, *Stochastic models that separate fractal dimension and the hurst effect*, SIAM Review, 2004, vol. 46, no. 2, pp. 269–282.

[6] M.M. Kanafi, *Surface generator: artificial randomly rough surfaces*, 2016.

[7] B. Persson, O. Albohr, U. Tartaglino, A. Volokitin, E. Tosatti, *On the nature of surface roughness with application to contact mechanics, sealing, rubber friction and adhesion*, J. Phys.: Condens. Matter, 2005, vol. 17, no. 1, pp. R1–R62.

[8] A. Duparré, J. Ferre-Borrull, S. Gliech, G. Notni, J. Steinert, J.M. Bennett, *Surface characterization techniques for determining the root-mean-square roughness and power spectral densities of optical components*, Appl. Opt., 2002, vol. 41, no. 1, pp. 154–171.

[9] T.D.B Jacobs, T. Junge, L. Pastewka, *Quantitative characterization of surface topography using spectral analysis*, Surf. Topogr.: Metrol. Prop., vol. 5, no. 1, art. no. 013001.

[10] D.S. Dugdale, *Yielding of steel sheets containing slits*, J. Mech. Phys. Solids, 1960, vol. 8, no. 2, pp. 100–104.

[11] J.H. Rose, J. Ferrante, J.R. Smith, *Universal binding energy curves for metals and bimetallic interfaces*, Phys. Rev. Lett., 1981, vol. 47, no. 9, pp. 675–678.

[12] N. Prodanov, W.B. Dapp, M.H. Müser, *On the contact area and mean gap of rough, elastic contacts: Dimensional analysis, numerical corrections, and reference data*, Tribology Letters, 2014, vol. 53, no. 2, pp. 433–448.

[13] M. Frigo, S.G. Johnson, *The design and implementation of FFTW3*, Proc. IEEE, 2005, vol. 93, no. 2, pp. 216–231.

[14] C. Campañá, Martin Müser, *Contact mechanics of real vs. randomly rough surfaces: A green's function molecular dynamics study*, Europhysics Letters, 2007, vol. 77, no. 3, art. no. 38005.

[15] S.P Venugopalan, L. Nicola, M.H Müser, *Green's function molecular dynamics: including finite heights, shear, and body fields*, Modelling and Simulation in Materials Science and Engineering, 2017, vol. 25, no. 3, art. no. 034001.

[16] S.P. Venugopalan, N. Irani, L. Nicola, *Plastic contact of self-affine surfaces: Persson's theory versus discrete dislocation plasticity*, J. Mech. Phys. Solids, 2019, vol. 132, art. no. 103676.

[17] Y. Murugesan, S.P. Venugopalan, L. Nicola, *On sub-surface stress caused by contact roughness in compressible elastic solids*, Tribology International, 2021, vol. 159, art. no. 106867.

[18] M. Khajeh Salehani, N. Irani, L. Nicola, *Modeling adhesive contacts under mixed-mode loading*, J. Mech. Phys. Solids, 2019, vol. 130, pp. 320–329.

[19] J.S. van Dokkum, M. Khajeh Salehani, N. Irani, L. Nicola, *On the proportionality between area and load in line contacts*, Tribology Letters, 2018, vol. 66, no. 3, art. no. 115.

[20] J.S. van Dokkum, F. Pérez-Ràfols, L. Dorogin, L. Nicola, *On the retraction of an adhesive cylindrical indenter from a viscoelastic substrate*, Tribology International, 2021, vol. 164, art. no. 107234.

[21] S. Sukhomlinov, M. Müser, *On the viscous dissipation caused by randomly rough indenters in smooth sliding motion*, Applied Surface Science Advances, 2021, vol. 6, art. no. 100182.

[22] J.S. van Dokkum, L. Nicola, *Green's function molecular dynamics including viscoelasticity*, Modelling and Simulation in Materials Science and Engineering, 2019, vol. 27, no. 7, art. no. 075006.

УДК 531-2:531-3:531.43:531.01:53.043:538.951

Последние достижения и методы контактной механики твердых тел с поверхностной шероховатостью и с использованием технологии Green's Function Molecular Dynamics

И. Соловьев[1], В. Петренко[1], Y. Murugesan[2], Л. Дорогин[1]

[1] Университет ИТМО, Санкт-Петербург, 197101, Россия
[2] Department of Industrial Engineering, University of Padova, I-35131, Italy

Аннотация. Несмотря на важность трибологии твердых тел с шероховатостью поверхности, на данный момент нет обобщенной теории адгезии. Один из способов описания адгезии в трибологических системах — метод Green's Function Molecular Dynamics (GFMD). Целью данной работы является обзор последних достижений в области контактной механики и приложений GFMD в контактной механике. Существуют различные атрибуты этого метода, важные для его реализации: модель для описания шероховатости поверхности, модель для описания межфазных сил, конститутивная модель для описания твердых деформаций и алгоритм минимизации энергии. В данном обзоре рассмотрен следующий набор параметров: степени свободы смоделированной системы, геометрия подложки, тип управление нагрузкой, свойства материала, топография поверхности, модели межфазного взаимодействия.

Ключевые слова: контактная механика; шероховатость поверхности; Green's function molecular dynamics; адгезия; трение